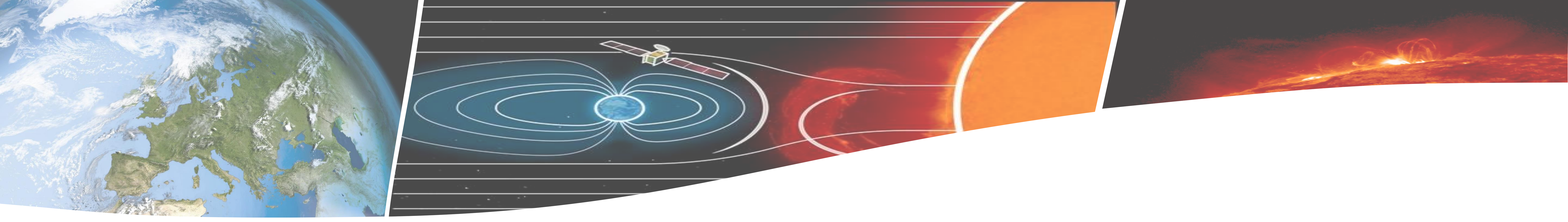

Ionospheric model validation using COSMIC 2 Preliminary results

Joana Morgado Pereira (joana.piresmorgadofernandespereira@dlr.de), Claudia Borries (claudia.borries@dlr.de), Frank Heymann (Frank.Heymann@dlr.de), Isabel Fernandez Gomez (Isabel.FernandezGomez@dlr.de) - Institute of Solar-Terrestrial Physics, German Aerospace Center, Neustrelitz, Germany.

Michael Schmidt (mg.schmidt@tum.de) - Deutsches Geodätisches Forschungsinstitut (DGFI-TUM), TUM School of Engineering and Design, Technical University of Munich, Munich, Germany.

Introduction

Space weather events (SWE) that result in geomagnetic storms influence electromagnetic wave propagation in the Earth's ionosphere and atmosphere, affecting communications, navigation, and positioning. Forecasting the state of the upper atmosphere and conditions following SWE is one of the key aspects to protect the current high technological society. However, accurately representing the thermosphere-ionosphere (TI) system is challenging due to its complex interactions with the lower atmosphere and the magnetosphere that are challenging to correctly represent. SWE events have often been poorly observed which can lead to uncertain conclusions about these phenomena. TI modeling is essential for understanding the complex coupling interactions between thermosphere and ionosphere to predict and mitigate SWE effects. Model validation is crucial to assess the capabilities of these models and to develop new modelling techniques. It shows the model's performance and identifies errors which can be caused by factors such as the solar cycle, daily or seasonal variability and other biases. So far, there is no standard set of validation tools or reference datasets that can be used in the TI domain. In this work Ionospheric radio occultation data (electron density) from COSMIC2 mission serves as the basis for validating the two models, (1) International Reference Ionosphere (IRI) and (2) the Thermosphere-Ionosphere-Electrodynamics General Circulation Model (TIEGCM). A set of verification and statistical methods is used to evaluate these models under various conditions (geomagnetically quiet and active) and periods (seasonal variations).

Data/Methods

- **Observations: Ionospheric Radio Occultation (IRO) Electron density (Ne)**

COSMIC-2 produces 5,000 vertical profiles per day (see Fig. 1.)
ref : https://www.cosmic.ucar.edu/what-we-do/cosmic-2/data
The data used for this work are the Ne Profiles obtained by inversion of calibrated TEC data, assuming spherical symmetry of the atmosphere. This causes significant errors below the F layer (such as large negative values of Ne). For this reason, data was bounded between 150-600km (see Algorithms for inverting radio occultation signals in the ionosphere at CDAAC).

- **IT models**
  - International Reference Ionosphere (IRI) - Empirical, ref : https://github.com/space-physics/iri2016
  - Thermosphere-Ionosphere-Electrodynamics General Circulation Model (TIEGCM) - Physics based, ref : https://www.wdc-climate.de/ui/entry?acronym=OTHITACS_tiegcm_2020

- **Six events are chosen:**
  - four during 72 quiet hours that correspond to the equinoxes and solstices of 2020: 20-22 of March, 20-22 of June, 22 to 24 of September and 21 to 23 of December.
  - one during a storm period: 25-30 of September 2020
  - The Dst index from OMNI was used to identify quiet (Dst > -50nT) or disturbed (Dst < -50nT) times (See Fig.2.)

- **Validation metrics:**
  - Plotted profiles and Model vs Observation plots.
  - Mean error (ME) where Error is defined as E = (model-data)/data
  - NmF2 and HmF2 from the data and the model
  - ΔNmF2 = NmF2(model)-NmF2(data)
  - ΔHmF2 = HmF2(model)-HmF2(data)

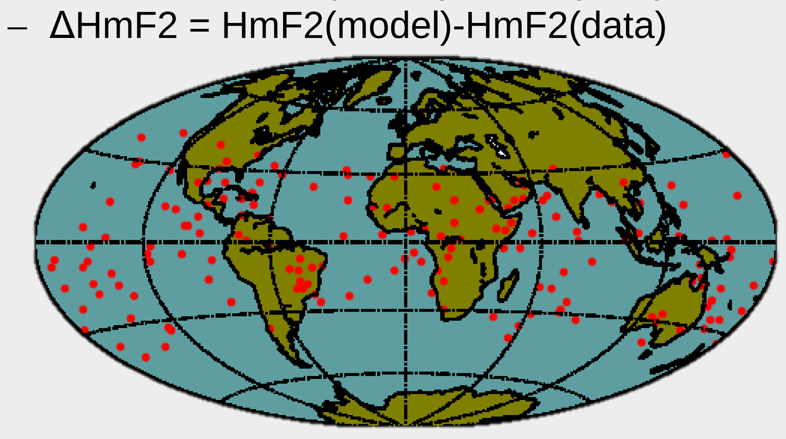

Fig.1. COSMIC2 coverage for the data used

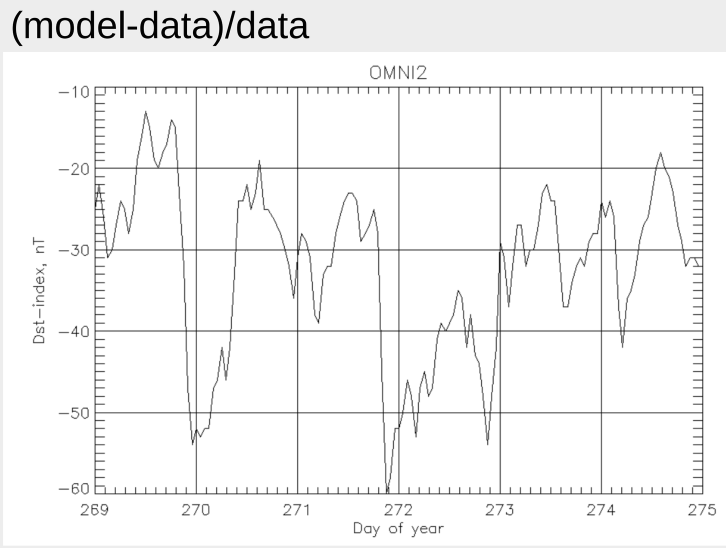

Fig. 2. Dst index during the disturbed period (25-30 September 2020)

Results

The results presented here are preliminary. The figures and tables were made in Python with downloaded data from COSMIC2 repository, TIEGCM dataset and IRI model runs.

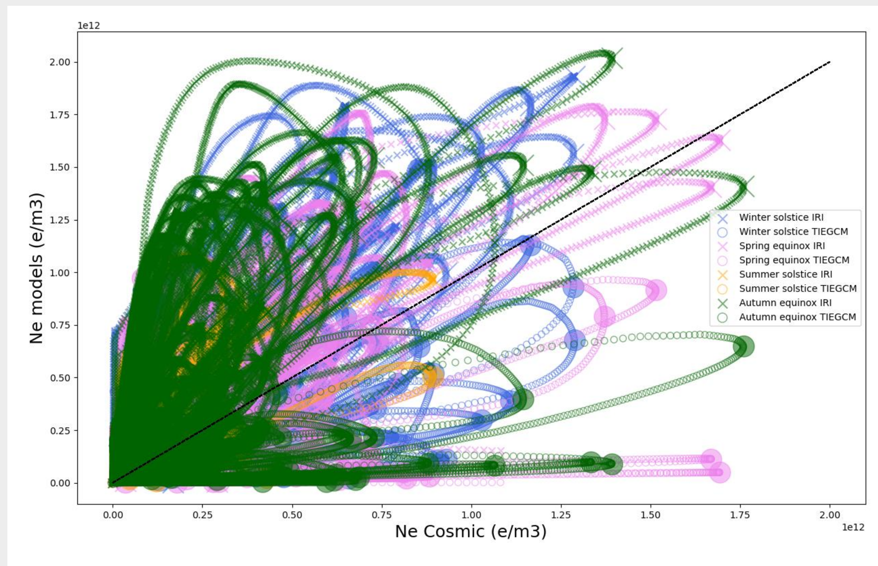

Fig. 3. Scatter plot between modeled vs observations during all quiet periods. Larger dots and crosses represent the maximum model Ne for observed NmF2

Table 1. Validation metrics for the two models analysed

Metric	ME		NmF2 ($x10^{11}$) and (ΔNmF2)			HmF2 (km) and (ΔHmF2)		
Date	IRI	TIEGCM	Cosmic2	IRI	TIEGCM	Cosmic2	IRI	TIEGCM
March	2.35	2.30	5.04	8.31 (3.27)	3.52 (-1.51)	256	286 (29.55)	285 (28.76)
June	5.35	3.46	2.21	5.39 (3.18)	2.23 (-0.01)	267	288 (21.13)	264 (-2.75)
September	5.27	2.87	4.37	10.87 (6.50)	2.47 (-1.89)	266	290 (23.30)	278 (11.70)
December	3.98	2.10	5.19	10.22 (5.03)	4.15 (-1.04)	289	297 (8.23)	299 (10.63)
27.09 (11h)	3.49	7.08	2.71	7.74 (5.03)	10.20 (7.49)	238	285 (47)	317 (79)
27.09 (13h)	2.28	0.99	1.95	5.64 (3.69)	5.04 (3.09)	228	257 (29)	253 (25)
27.09 (20h)	2.50	-0.64	3.06	10.59 (7.53)	0.96 (-2.10)	244	271 (27)	290 (46)
27.09 (23h)	0.21	-0.46	7.97	12.86 (4.89)	7.63 (-0.34)	330	360 (30)	302 (-28)

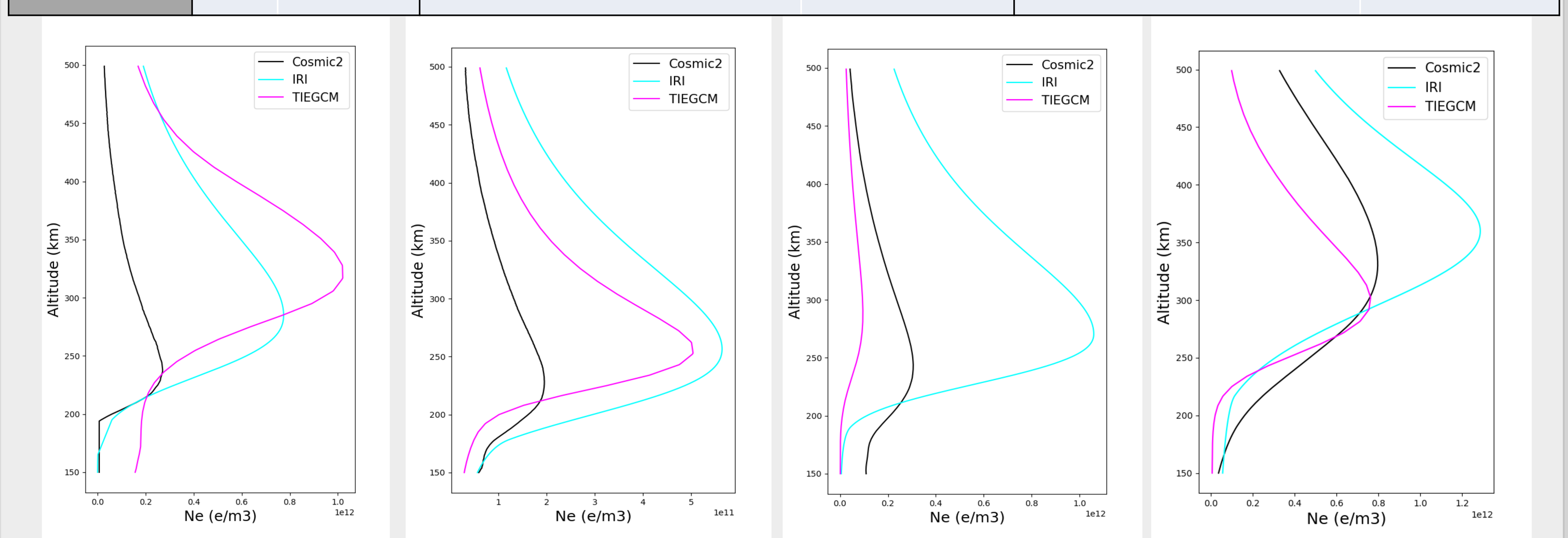

Fig. 4. Observed and modeled (IRI and TIEGCM) Ne profiles on the storm day (27 September 2020) from left to right: before the storm (11h), sudden storm commencement (13h), main storm phase (20h), recovery phase (23h)

Discussion and Conclusion

Looking at the scatter plot of Model vs Observation in the quiet periods, (see Fig. 1.) there is a bias seen in both models, IRI mostly overestimates, being above the black line (x=y line) and TIEGCM underestimates the observations. From the ME in Table 1 it can be seen that TIEGCM is in general more accurate than IRI in all quiet events. It is expected that the accuracy of both models is lower in disturbed events, however only one profile per hour is here represented. For this single event TIEGCM preforms better taking into consideration ME in all cases except in the hours prior to the storm (11h). In the two last columns of Table 1. the observed NmF2 and HmF2 are compared with the modeled ones, and their difference (ΔNmF2 and ΔHmF2) is calculated. TIEGCM presents values for the density and altitude of F2 closer to the ones observed for the quiet periods, comparing with IRI. As for the storm hours, both models worsen their performance in predicting the altitude and density of the F2 layer. The performance of the models during the four storm periods can also be compared using the profile plots in Fig.4. Concluding, the model's ability to reproduce an Ne profile could be correlated to how well the model represents the peak of the F2 layer.

The study presented here shows that simple statistics and metrics can be the basis for a comprehensive model validation framework. It covers the accuracy, bias and predictability of NmF2 and HmF2, making it simple to compare different models. As future work it is proposed that more models are evaluated in this way and that cross validation with other data sources and models is done. Furthermore more periods of geomagnetic activity should be considered such as solar cycles, solar rotations and other geomagnetic storms with different origin, duration and intensity. A validation framework is being developed with the goal to serve the evaluation of a model ensemble.

References: Chou, M.-Y et. al. (2023) "Validation of Ionospheric Modeled TEC in the Equatorial Ionosphere During the 2013 March and 2021 November Geomagnetic Storms" | A. T. Chartier et. al. (2023) "Validating Ionospheric Models Against Technologically Relevant Metrics" | Francisco J. Tapiador and Vincenzo Levizzani, (2021) "2.3 Climate Model validation" | H. Wang, (2008) "Validation of the Space Weather Modeling Framework using observations from CHAMP and DMSP" | K.A. McWilliams R.G. Harrison K.A. Nicoll, (2013) "Space weather driven changes in lower atmosphere phenomena" | JA Guerra, SA Murray, and E Doornbos, (2020) "The use of ensembles in space weather forecasting"| A. Pignalberi, D. Bilitza, P. Cosson et al., Validation of the IRI-2020 topside ionosphere options through in-situ electron density observations by low-Earth-orbit satellites, Advances in Space Research | Shaikh, M. M., Nava, B., & Haralambous, H. (2018). On the use of topside RO-derived electron density for model validation. Journal of Geophysical Research: Space Physics, 123, 3943–3954.